PCCP

Carboxylate Binding Prefers Two Cations to One

Journal:	*Physical Chemistry Chemical Physics*
Manuscript ID	CP-ART-08-2022-003561.R1
Article Type:	Paper
Date Submitted by the Author:	30-Aug-2022
Complete List of Authors:	Stevens, Mark; Sandia National Laboratories, Rempe, Susan; Sandia National Laboratories

Journal Name

ARTICLE TYPE

Cite this: DOI: 10.1039/xxxxxxxxxx

Received Date
Accepted Date

DOI: 10.1039/xxxxxxxxxx

www.rsc.org/journalname

Carboxylate Binding Prefers Two Cations to One†

Mark J Stevens,*[a] and Susan L. B. Rempe,[a,b†]

Almost all studies of specific ion binding by carboxylates (-COO^-) have considered only a single cation, but clustering of ions and ligands is a common phenomenon. We apply density functional theory to investigate how variations in the number of acetate ligands in binding to two monovalent cations affects ion binding preferences. We study a series of monovalent (Li^+, Na^+, K^+, Cs^+) ions relevant to experimental work on many topics, including ion channels, battery storage, water purification and solar cells. We find that the preferred optimal structure has 3 acetates except for Cs^+, which has 2 acetates. The optimal coordination of the cation by the carboxylate O atoms is 4 for both Na^+ and K^+, and 3 for Li^+ and Cs^+. There is a 4-fold coordination minimum just a few kcal/mol higher than the optimal 3-fold structure for Li^+. For two cations, multiple minima occur in the vicinity of the lowest free energy state. We find that, for Li, Na and K, the preferred optimal structure with two cations is favored over a mixture of single cation complexes, providing a basis for understanding ionic cluster formation that is relevant for engineering proteins and other materials for rapid, selective ion transport.

1 Introduction

The structure of ions in molecular systems is a fundamental phenomenon that controls the behavior of many systems. Ion binding is important in determining not just static structure, but also the dynamics of ion transport.[1–3] Such ion dynamics are important in a wide range of applications including energy storage,[4–6] water filtration,[7,8] ion channel proteins[9–12] and perovskite solar cells.[13,14] Accurate characterization of the binding between ligands and ion can be done using density functional theory (DFT) methods.[15,16] Almost all density functional theory (DFT) calculations have treated binding of a single ion, but most systems involve more than one ion. Given that the constraints of the binding geometry play an important role in binding selectivity, determining the binding constraints with more than one ion is especially relevant. Here, we present a new computational study of binding of the carboxylate group to two ions for a series of monovalent ions.

In this paper, we focus on the carboxylate functional group (-COO^-), which is ubiquitous in biological[17,18] and synthetic molecules.[19,20] Specifically, we treat the acetate ion as the ligand. In biological ion channels[9,21] and synthetic ionomers,[22] carboxylates may form binding sites that solvate simple metal ions and lower free energy barriers to ion conduction. Because either one (mono-) or two oxygens (bi-dentate) in a carboxylate may participate in binding, the geometry of the coordination is important. In our previous paper,[16] we addressed the binding of carboxylate ligands to a single metal ion and introduced the theory of architectural constraints[2,11,23–25] applied to this problem. The architectural constraints theory resolves two competing hypotheses for the (inverse) Hofmeister series.[26–28] According to the 'ligand field strength' hypothesis, higher anionic field strength of a binding site should favor smaller over larger cations.[29] According to the 'equal affinities' hypothesis,[30] entities with matching hydration free energies tend to associate. Our results supported the ligand field strength hypothesis and followed the reverse Hofmeister series for ion solvation and ion transfer from aqueous solution to binding sites with the preferred number of ligands. In addition, a key insight insight arose from the finding that ion-binding sequences can be manipulated and even reversed just by constraining the number of carboxylate ligands in the binding sites. In other words, architectural contraints of the ligands are determining factors in ion binding.

In the present work, we treat the binding of carboxylate ligands to two identical monovalent metal ions in the series Li, Na, K, and Cs. We determine the lowest binding free energy for the gas phase with a variable number of ligands and determine whether the preferred ligand composition changes for two ions in comparison with just one ion. We find how the ligand geometry changes, in terms of mono- and bi-dentate binding under the constraint of

[a] Center for Integrated Nanotechnologies, Sandia National Laboratories, Albuquerque NM 87185, USA
* E-mail: msteve@sandia.gov
[b] CBRN Defense and Energy Technologies, Sandia National Laboratories, Albuquerque, NM, 87185
† E-mail: slrempe@sandia.gov

† Electronic Supplementary Information (ESI) available: [Images of additional geometries of near optimal structures, table of ΔG values and tables of distances are given.]. See DOI: 00.0000/00000000.

having two ions. Finally, we address whether an ion complex with two cations has a lower free energy than two complexes with one ion.

2 Methods

The local clustering of acetate ligands in a two ion complex corresponds to the following reaction,

$$2X^+ + n\mathrm{CH_3COO^-} \rightleftarrows (\mathrm{X^+})_2(\mathrm{CH_3COO^-})_n, \quad (1)$$

where X^+ indicates a monovalent ion binding with n=1 to 4 charged acetate ligands (CH_3COO^-) to form an ion-acetate complex, $(X^+)_2(CH_3COO^-)_n$. We assume the clustering equilibria take place in an idealized environment that does not influence the reaction through long-ranged dispersive and electrostatic interactions or other structural constraints on the clusters. Our treatment is thus equivalent to an uncoupled quasi-chemical analysis carried out in a low dielectric environment (ε=1).[31,32]

We calculated the free energy change (ΔG) for the reactions in Eq. 1 using the Gaussian 16 quantum chemistry package.[33] To calculate the free energy change for the reactions in Eq. 1, we took the difference in free energy between the product (p) and the sum of the reactants (r) in stoichiometric proportions (n_r):

$$\Delta G = G_p - \Sigma n_r G_r. \quad (2)$$

For most systems, the geometry optimizations were carried out in the gas phase using the density functional theory approach with the hybrid B3LYP approximation to the exchange-correlation energy[34] and Dunning's correlation-consistent polarized double-zeta basis sets augmented with diffuse functions (aug-cc-pvDz).[35,36] Previous DFT calculations for Li^+ and Na^+ found this combination of functional and basis set to be sufficiently accurate.[16,37,38] The B3LYP functional is the most widely used approximation in chemistry due to its balance between computational efficiency and ability to describe strongly interacting systems.[39] We also performed some calculations using the ωB97X-D functional,[40] which has been found to work well in a study of the dispersion and exchange-corrected DFT for Na^+ hydration.[41] We will focus on the B3LYP results as the free energies for Li^+ and K^+ using ωB97X-D yielded similar free energy dependence as B3LYP. Correlation-consistent basis sets were developed to describe core-core and core-valence electron correlation effects in molecules and previously have been shown to be accurate for a single carboxylate.[37] For Cs^+, we used the LANL2DZ effective core potential and valence electron basis set for computational efficiency.[42]

Previously, we found that the the basis set superposition error (BSSE) correction of the interaction energy by the counterpoise method was not significant,[16,41] and therefore have not performed the calculation here. To obtain free energies, we performed a normal mode frequency analysis[43] using the same level of theory as for optimization. Stable structures for which the forces are zero and frequencies positive confirmed true minima on the potential energy surfaces. The thermodynamic analysis yielded zero point energies and thermal corrections to the electronic energy due to translational, electronic, and vibrational motions calculated at a temperature of 298 K and pressure of 1 atm. The values of G in eq. 2 are the sum of the electronic energy and the thermal energies.

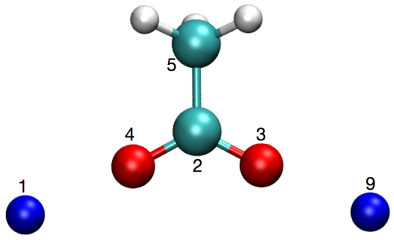

Fig. 1 Optimized configuration for a single acetate with two Na atoms. Atom labels are used for distances in Table S2. Colors: C cyan, O red, H white and Na blue. Images made using VMD.[44]

3 Results

We first discuss the optimized structures as a function of the number of acetates n for the different cations. Across the different cations there are some similarities in the geometries, but also there are significant differences. Cs^+ is particularly distinct from the other three cations. In the case of a single cation, the cations prefer a tetrahedral coordination by the carboxylate O atom, which requires two acetates to achieve. A common motif of the local binding geometry is the bidentate and the monodentate geometries for binding of individual carboxylates to the cation. The optimal binding to two cations may put additional constraints on the positioning of the acetates, which affects the possible binding geometries. When there are enough ligands, we find the tetrahedral coordination of individual cations occurs, but we also find 3-fold coordination is favored in some cases. In addition, we found that for $n > 1$, there can be multiple minima with small differences in the free energies (even less than 1 kcal/mol). These occur because there are similar, but different geometries for minimizing the repulsion between like-charged atoms and maximizing the attraction between oppositely charged atoms.

We discuss next the lowest free energy structures for number of ligands in the range $n = 1$ to 4. All attempts to optimize a stable structure for $n = 5$ or 6 led to structures with at most 4 acetates in the first solvation shell and other ligands out in a second shell.

3.1 Optimized Structures

The optimized structures for a single ligand binding two cations are simple. A cation is collinear with each of the C-O bonds, as shown in Fig. 1 for the Li cation. The main difference among the cations is that the distances between the cations and the O atoms r_{XO} increase with the ion size (see Table S2).

For two ligands, the optimized geometries are similar, but Li exhibits small but structurally significant differences from the others. Fig. 2 shows the optimized geometries for Li and Na. The geometry for K and Cs match that of Na with primarily the distances between the cation and O atoms increasing (see Table S3). The cations and the carboxylate groups are coplanar in all cases. For Na each acetate is close to a bidentate geometry with one of the cations. In addition, each acetate has one O atom that also binds to the other cation. This arrangement gives a 3-fold

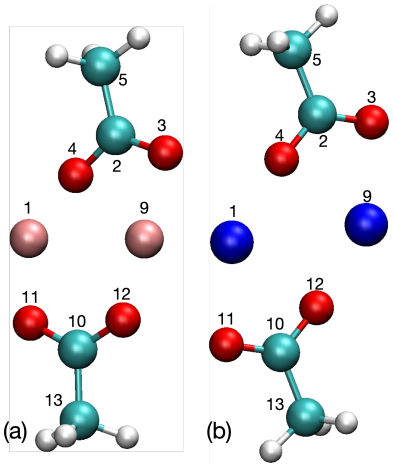

Fig. 2 Optimized configuration for two acetates ($n = 2$) with (a) two Li and (b) two Na atoms. Atom labels are used for distances in Table S3. The structures for K and Cs are similar to the Na case. Colors: C cyan, O red, H white, Li pink and Na blue.

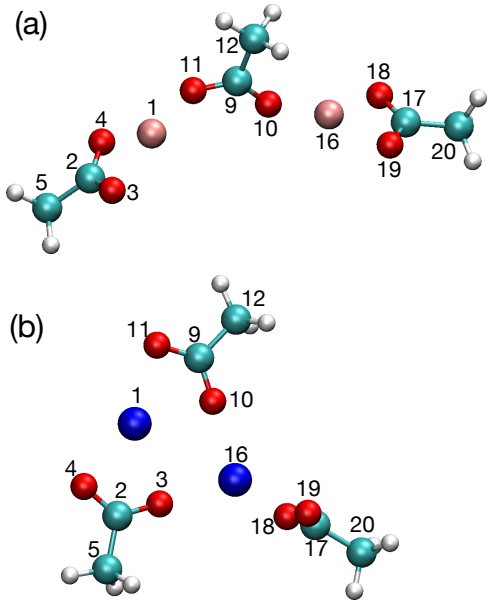

Fig. 3 Optimized configuration for three acetates ($n = 3$) with (a) two Li and (b) two Na atoms. Labels are used for distances in Table S4. Colors: C cyan, O red, H white, Li pink and Na blue. The optimized geometries for K and Cs are similar to the Na structure.

coordination for each cation, which does well at minimizing the electrostatic energy for the planar geometry. With just 2 acetates it is not possible to have a low energy 4-fold coordination. To get 4-fold coordination, the two acetates would have to form a bidentate complex with one of the cations and the other cation secondarily bind to one or more O. This structure does not have a low energy.

An examination of the cation-O distances in Table S3 reveals that the optimal structure for a single ligand binding two cations is not a symmetric bidentate geometry. In a symmetric structure the 9:4 and 9:3 distances would be the same, but they are slightly different, because the O atom 4 is shared between the two cations. Similarly, the 1:11 and 1:12 distances are not the same. Instead, both the 9:4 and 1:12 distances are the same, and the 9:3 and 1:11 distances are separately identical. In addition, the 1:4 and 9:12 distances are the same. This bidentate structure gets distorted, because in each acetate one O binds to only one of the cations, while the other O atom binds to both cations. Overall, the geometry has multiple congruent parts, which occurs by slight adjustment of the bidentate geometry. The K and Cs optimized geometries are topologically equivalent to the Na geometry. The main difference is the cation O distances increase with ion size.

In contrast to the other cations, the binding geometry for the Li cations has only one bidentate binding mode. The Li atom (1 in Fig. 2) is monodentate to each of the acetate ligands. This arrangement results in one Li being 3-fold coordinated, and the other being only two-fold coordinated. This structure is a slight shift from the minimum energy structure found for the other cations, as can be seen by comparing the two images in Fig. 2. For the Li system, a minimum was found for the near double bidentate structure similar to the other systems, but the free energy is 1.1 kcal/mol higher than the structure in Fig. 2a. In a condensed system, this free energy difference is small enough that both structures would occur in the distribution of structures.

Increasing the number of acetates to three enables 4-fold coordination of both cations for Na (as shown in Fig. 3), K and Cs. For these cations, the three carboxylates are bidentate and two carboxylates have an O atom that additionally binds to the other cation. With this geometry, all the Na:O distances are almost the same at about 2.30 Å with the variation being -0.01 to +0.05 Å. The main difference among these three ions is again that the cation:O distances increase with ion size.

The lowest free energy structure for Li is different with two acetates being bidentate, and the middle one being monodentate to each Li^+. The Li^+ are 3-fold coordinated in this geometry. In this structure the monodentate Li:O distance is shorter than the bidentate separation by 0.27 Å, which yields a stronger electrostatic interaction for the monodentate bonds. There is a minimum for a 4-fold coordinated Li structure like that for Na that is only 1.3 kcal/mol higher in free energy. The 3-fold coordinated, lowest free energy structure has a large Li:Li separation distance of 5.03 Å, which lowers the cost of the Li:Li repulsion. In the higher energy 4-fold coordinated structure, the Li:Li separation distance is smaller at 2.74 Å, and the Li:O separations are slightly smaller than the bidentate separations in the 3-fold structure, but not the monodentate separations. Thus, there is a trade off between Li:Li repulsion and Li:O attractions, and for Li the 3-fold structure has the lowest energy.

At $n = 4$, there are more than enough O atoms to form two separate 4-fold coordinations of the two cations. Na, K, Cs have each cation 4-fold coordinated (see Fig. 4(b)). The lowest free energy Na structure is slightly different with one Na:O has a large separation (see 1:10 in Table S5). An alternate minimum energy structure for Na exists that is more similar to the K/Cs structures, but with a slightly higher free energy (1.3 kcal/mol). In all these structures, two of the acetates are separately bidentate with one of the cations, and the other two acetates are separately mon-

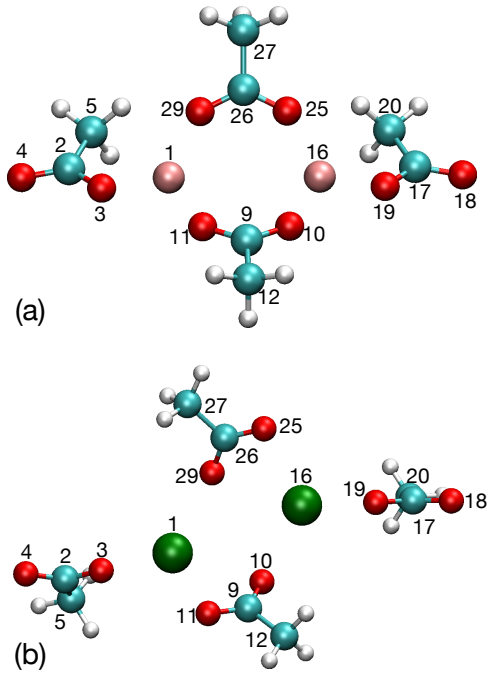

Fig. 4 Optimized configuration for four acetates ($n = 4$) with (a) two Li and (b) two K. Labels are used for distances in Table S5. The optimized structures for Na and Cs are similar to the K structure, but the 1:10 distance is large. See text and Table S5 for differences. Colors: C cyan, O red, H white, Li pink and K green.

odentate with one of the cations. The two bidentante binding acetates also have a monodentate binding to the other cation to obtain the 4-fold O coordination of the cations.

In contrast to other ions, the Li optimized structure has both cations 3-fold coordinated with all the acetates binding in monodentate mode. Two of the acetates singly bind to both cations and two only bind to one each of the Li^+. In this geometry, the Li:Li separation (Table S5) is larger than the Na:Na separation, which is related to the cost of the electrostatic repulsion between two cations. The 4-fold coordinated Na structure has shorter Na:Na separation by compensating the cost of the Na:Na repulsion with better Na:O attraction and a more compact structure with alternating positive and negative charges. Optimization of the Li system at $n = 4$, using the 4-fold coordinated structure with adjusted Li:O separations, did not yield a distinct minimum energy state with a 4-fold structure.

In Table 1, we summarize the coordination of the cations as a function of n and the cation type. When a sufficient number of ligands occurs, 4-fold coordination is preferred. Li is the outlier with lower coordination. We note that alternate minimum energy structures were also obtained and the energy difference with the optimal case was typically small, a few kcal/mol. Thus, in condensed system these structures would all coexist, because thermally they all would be accessible.

The separation distance r_{XX} between the two cations shown in Fig. 5(a) has interesting behavior as a function of cation. For $n = 1$ and 2, the sequence matches the ion size. At $n = 3$, the order changes, because Li is only 3-fold coordinated and the Li:Li separation is the largest. For the other ions, the separation increases with ion size. For $n = 4$, Li is again out of order, but this time the Li:Li separation is only larger than the Na:Na separation.

The magnitude of r_{XX} as a function of n has interesting behavior. Going from a single to two ligands, the cation separation drops significantly. At $n = 2$, the screening by the 4 O atoms is sufficient to allow the two cations to be much closer than for a single ligand, where the cations separate as much as possible to reduce their repulsion while still being bound to one of the O atoms. Increasing n to 3 results in a slight increase in r_{XX}, except for Li. Similarly, there is a slight increase going to $n = 4$, although here Na has a larger increase, as noted above. This behavior is important for the comparison of two-cation complexes vs. one-cation complexes, which we will address below.

The oxygen-cation separation distance r_{OX} is shown in Fig. 5(b). There are multiple points for a given oxygen-cation pair as each binding pair has a value on the plot. The $n = 3$ case visually stands out because there is little scatter in the r_{OX} for a given cation, especially in comparison to $n = 2$ and 4 (for $n = 1$ there are two identical values and no scatter). This lack of scatter is due to the 4-fold coordination with high symmetry; the exception Li has more scatter. For the most part, the values of r_{OX} show ion size ordering (Cs > K > Na > Li). One exception at $n = 2$ is the large O:Li separations at 2.86 Å, which is the 1:12 pair in Fig. 2(a). This pair is really not a binding pair and could be removed from the figure, but the fact that this value is above the K values demonstrates that the pair is much different than the others, which are binding pairs. Similarly, at $n = 4$ there is the Na r_{OX} at 3.60Å which is the 1:10 pair in Fig.4 which is the stretched bond. As a function of n, the lowest values are for $n = 1$. For larger n the average value is increases a small amount compared to the $n = 1$ value; the scatter is a more significant quantity.

3.2 Complexation Free Energy

Now that we have determined the optimized structures, we consider the solvation free energy ΔG shown in Fig. 6 as a function of n and cation type. We see the same ordering of ΔG as a function of cation type as found earlier for the free energy of binding to a single cation, namely Cs > K > Na > Li. The preferred ligand composition is $n^* = 3$ for Li, Na and K. For these cations, the free energies just one off from the preferred ligand composition are about 30 kcal/mol higher. Thus, there is a substantial difference between the preferred ligand composition and the next best number of ligands in these cases. Cs is an exception; the preferred ligand composition is $n^* = 2$ and this state is just 5.8 kcal/mol lower than $n = 3$.

The optimal structures at the preferred ligand composition n^*

Table 1 Optimal coordination of the two cations.

n^a	Q^b	Li		Na		K		Cs	
1	1	1	1	1	1	1	1	1	1
2	0	2	3	3	3	3	3	3	3
3	-1	3	3	4	4	4	4	4	4
4	-2	3	3	4	4	4	4	4	4

[a] Number of acetates [b] Total charge

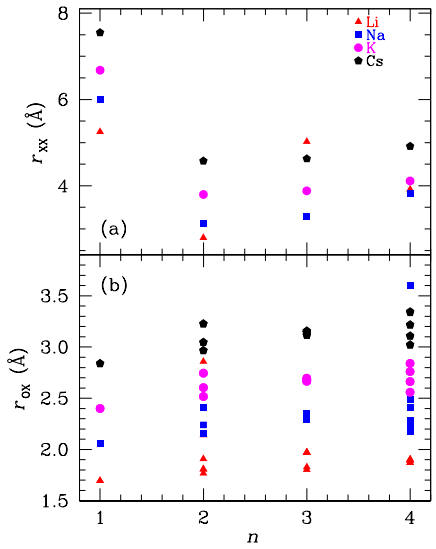

Fig. 5 (a) The cation-cation (X-X) distance for each cation and number of ligands n. For n with the two structures close in ΔG, both values are plotted. (b) The cation-O atom distances for each cation and n. Every case of r_{OX} for a given cation and n is plotted. See tables S1-S4 for values.

involve either 3 or 4-fold coordination of the cations by O atoms. At $n^* = 3$ for Na and K, the optimal structure has both cations 4-fold coordinated by the O atoms. Li has only one cation 4-fold and the other 3-fold coordinated, but Li has the lowest free energy of all the cations. The Li:O separations are the shortest of all the cations. This arrangement along with the largest Li:Li separation, contributes to a very negative electrostatic energy. Since Cs has $n^* = 2$ for the preferred ligand composition, both cations are 3-fold coordinated. The largest cation-oxygen separations for Cs^+ yield the highest ΔG.

4 Discussion

Our previous results for single monovalent cation binding by carboxylates in acetates found tetrahedral coordination to be the lowest free energy structure, except for Cs, which has 6-fold coordination as the lowest free energy structure. We find 4-fold coordination also preferably occurs in binding of two cations, with number of ligands shifting to $n^* = 3$ for Na and K. At $n^* = 3$, there are a sufficient number of carbonyl O atoms to provide the tetrahedral coordination of both cations. For Li the preferred structure is 3-fold coordinated with $n^* = 3$ acetates, although there is a minimum energy 4-fold structure with a free energy slightly above. The Li:O separations are the shortest of all the cations studied, resulting in stronger attractions. Combined with a large Li:Li separation, the 3-fold structure has a lower energy albeit by a small amount. In all these systems, the low energy structure is an optimization of maximizing the cation-O attraction while minimizing the cation-cation repulsion. There are multiple free energy minima, because there are coordination geometries in which the ionic spacings vary significantly, but differ in free energies by only a few kcal/mol. Finally, Cs again is different from the other cations with $n^* = 2$ with 3-fold coordination. Also, in contrast to the other cations, the free energy difference between that state and the optimal $n = 3$ state is not large (5.8 kcal/mol vs. about 30 kcal/mol). Overall, for all the cations the optimal structures at n^* possess a charge ordered structure with alternating positive (X^+) and negative ions (O^-) that yields highly negative free energies.

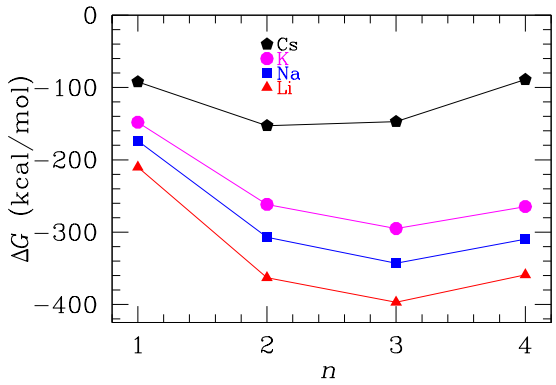

Fig. 6 The change in free energy (ΔG) for formation of ion-carboxylate complexes as a function of the number (n) of acetate ligands in a low dielectric environment ($\varepsilon = 1$). Numerical values for ΔG given in Table S1.

At the preferred number of ligands $n^* = 3$, the total charge is -1. This nonneutral value has significant implications for structures in condensed phases, which tend to have local neutral complexes. Moreover, for these system (Li, Na, K) with $n^* = 3$, the $\Delta\Delta G$ for $\Delta n = \pm 1$ is large, which precludes transitions to $n = 2$ with total charge of the complex $Q = 0$. The nonneutrality and the large negative ΔG for all n suggest that there will be a mixture of cluster sizes in condensed phases to achieve a net neutral system. A probable mixture would be of $n = 1$, $Q = +1$ and $n = 3$, $Q = -1$. The large $\Delta\Delta G$ implies that these local complexes would be rather stable and ion transport would have high barriers, resulting in low diffusion rates. Direct analysis of this prediction requires studying structures for 3, 4 and more cations.

In the limit of a large number of cations and acetate ligands, the crystal structure will be the lowest energy condensed states (ignoring the role of temperature here). Crystal structures provide the periodic structures of multiple cations binding to acetates. The common crystal structures of ion acetates are hydrated versions, since the crystals strongly absorb water, but there are some measurements on anhydrous crystals. The simplest crystal structure is for crystalline sodium acetate, which has two Na atoms in the unit cell, and the Na atoms are 6-fold coordinated by O atoms.[45] For cesium acetate the unit cell has 6 Cs atoms all of which are 8-fold coordinated by O atoms.[46] Lithium acetate crystal structures are more complicated. There are two anhydrous polymorphs for the lithium acetate crystal with 15 and 108 Li atoms in the unit cell, respectively.[47] For the 15 Li atom unit cell, there is more than one coordination for the Li atoms.

The crystal structure of sodium acetate has Na 6-fold coordinated, which is interesting in that it is different from the 4-fold structure for the two Na^+ optimal structure. In the crystal the local structure about the Na atom includes 4 monodentate acetates, with the binding O atoms in a plane above the Na atom.

One bidentate acetate is below the Na with the acetate perpendicular to the plane of monodentate O atoms. This structure has 5 acetates binding to a single Na. In a gas phase, the 5 acetate structure it is not stable, because there are too many negatively charged acetates and only one Na^+. Adding another Na^+ to the structure does not help much. In the crystal structure a second Na neighboring the first only binds to two of the monodentate acetates. This is not a low energy structure for two Na atoms. Overall, we can see that the structure of small clusters is not going to be similar to the crystal structure.

One question we can address is whether clusters containing a single cation are more or less favored that clusters with two cations. We can calculate the $\Delta\Delta G$ for the reaction

$$X^+(CH_3COO^-)_{m_1} + X^+(CH_3COO^-)_{m_2} \rightleftarrows X_2^+(CH_3COO^-)_n, \quad (3)$$

where $m_1 + m_2 = n$. In particular for $n = n^* = 3$ for Li, Na and K, then $m_1 = 2$ and $m_2 = 1$ is the only choice. The free energy difference is

$$\Delta\Delta G_{21} = \Delta G_2(3) - (\Delta G_1(2) + \Delta G_1(1)), \quad (4)$$

where ΔG_i(n) is the free energy of i cations with n acetates. For $n = n^* = 3$ with $m_1 = 2$ and $m_2 = 1$, we obtain $\Delta\Delta G(21) = -29.3$, -25.1 and -26.5 kcal/mol for Li, Na and K, respectively. Thus, the two-cation structure is preferred over the mixture of single cation structures at $n = n^*$. For Cs which has $n^* = 2$ and $m_1 = m_2 = 1$, $\Delta\Delta G(21) = +45.2$ kcal/mol and the single cation clusters are favored over the two-cation complex. In contrast, Li, Na and K all have the two-cation $n = 2$ complex favored over two single cation clusters. However, for $n = 4$ two single cation clusters each with 2 acetates ($m_1 = m_2 = 2$) are favored: $\Delta G(21) = +50.8$, +48.6 and +35.0 kcal/mol for Li, Na and K, respectively.

Thus, whether a complex with two cations is favored over clusters with a single cation each depends on the number of acetate ligands. At the most favored number of ligands for two cations, the single, two-cation structure is favored over a split into two clusters with a single cation each for Li, Na and K, but not for Cs, which has a smaller n^*. Increasing n above n^* results in the single cation clusters being preferred. This result implies for Li, Na and K that complexes with at least two cations will be most likely to form in condensed systems. For Li, recent experiments and molecular dynamics simulations find strong clustering, as implied by our results.[48] This work studied Li trifluoacetate in a concentrated solution of low-dielectric ether solvent and found strong clustering consistent with our results.

With respect to ion transport in the melt phase of ionomeric polymers, the very strong binding of carboxylates for two cations in the preferred state is far too stable and will trap ions. Thus, for fast ion transport there is the need for polymer structure that *prevents* formation of the optimal structure. While the backbone flexibility and spacing of charges along the backbone will constrain the ionic cluster structure, tightly bound clusters have been common in atomistic simulations of ionomers with carboxylates.[4,5] Carboxylates may simply be poor candidates for the ionic group. Interest has grown in recent years for the ionic group to come from ionic liquid molecules.[49] One aspect of ionic liquid molecular structure is that compact structures with high coordination of the ions is restricted by the larger bulk of the molecules. This facilitates ion binding that does not have a large barrier to rearrangement of ions and consequently fast ion transport. The other common alternative is to include solvent molecules even though removing the flammable solvent is one of the main goals. One effect of the solvent molecules is to provide alternate binding complexes with sufficiently low free energy barriers that yields good ion transport. We also note that Li is the most strongly bound of the cations, which makes it the most challenging of the ions to design molecular structures for fast ion transport.

Our results also have important implications for ion channels due to the observation here that the most preferred structure has two cations, which is favored over splitting into two separate single cation complexes for Li, Na and K. This suggests that ion channels with cations neighboring (i.e. no water between) are feasible with the geometry of the ion channel matching the optimal structures found here. We have not yet considered complexes involving both water and acetate (or other carboxylates and polar functional groups), and how the free energies change in the presence of water is to be determined. These results simply show that structures with two neighboring cations are stable. In fact, these optimal states are too stable to promote ion transport, which raises some questions for future research. For example, in potassium ion channels that catalyze rapid transport of K^+ involving polar functional groups in the ion permeation pathway, is the channel structure close to the optimal structure or constrained to a non-optimal configuration, and does it prefer neighboring K^+ ions that are not trapped, or is water necessary to prevent the K^+ from being trapped? Similar questions apply to ion channels with carboxylate functional groups in their permeation pathways, such as pentameric ligand-gated ion channels and channelrhodopsins.[50,51] Together with prior works,[2,21,52–57] studies like the ones presented here may help resolve those questions for ion transport channels in future work.

Water is present in biological systems and common in charged polymer systems, in general. The effect of water on the interactions of ions with carboxylates is important to address.[58] The ionic interaction between cations and the carboxylate group is stronger than the interaction with water, but one of the remaining questions is the nature of binding in the presence of multiple waters. Key questions for mixtures of waters, ions and acetates (or other anionic binding molecules) that are relevent for ion transport include what are the minimum energy cluster structures and what are the barriers between distinct structures. We plan to address these issues shortly.

5 Conclusions

To better understand the nature of binding between carboxylates and cations, we performed DFT calculations of the binding between two cations (Li, Na, K, Cs) and the carboxylate group in acetate ligands. The functional mechanisms in most material or biochemical systems typically involve multiple cations. We determined the extent of the constraints for binding more than one cation on the geometry and energy of the binding to multiple acetates. The most common preferred structural motif is tetrahe-

dral coordination of the cations by the O atoms in the carboxylate groups. For the acetate molecule, which is one of the smaller molecules with a carboxylate group, the tetrahedral binding is not prevented, but not preferred for all cations. For both Na and K cations, the lowest free energy state has 3 acetates binding to the two cations with both tetrahedrally coordinated by the carboxylate O atoms. For Cs, the optimal binding of 3 acetates is also tetrahedral, but the lowest free energy occurs for 2 acetates which have a 3-fold coordination. This observation is consistent with Cs being distinct from the other cations in binding to a single cation. Binding to Li is a bit of an outlier in that the lowest free energy state has 3 acetates, but they bind in a 3-fold coordination. However, there is a close minimum energy state ($\Delta\Delta G = 1.3$ kcal/mol) with 3 acetates binding to Li with 4-fold tetrahedral coordination. One difference between binding to two cations compared to a single cation is the presence of minimum energy states that are structurally and energetically close to the absolute minimum energy state. These states have key distinct structural features such as a difference in coordination that occurs by a rotation of a ligand, for example.

We also determined that the two-cation complexes for Li, Na, and K with 3 acetates has a lower free energy than two single cation complexes. Thus, it is possible for two cations to be favored to be neighbors in an ion channel, for example. In condensed systems, such as ion-containing polymer melts, this result implies that ion clusters with more than one cation are likely in carboxylate systems. The strong binding within these complexes imply that carboxylate-containing ionomers will not be good ion conductors because the ions will be trapped effectively in clusters. Architectural constraints of the ligands may be needed to reduce ion trapping and promote ion conduction.

Conflicts of Interest

There are no conflicts of interest to declare.

Acknowledgement

This work was performed, in part, at the Center for Integrated Nanotechnologies, an Office of Science User Facility operated for the U.S. Department of Energy (DOE) Office of Science. Sandia National Laboratories is a multimission laboratory managed and operated by National Technology & Engineering Solutions of Sandia, LLC, a wholly owned subsidiary of Honeywell International, Inc., for the U.S. DOE's National Nuclear Security Administration under contract DE-NA-0003525. We gratefully thank Sandia's Laboratory-Directed Research and Development program for funding. The views expressed in the article do not necessarily represent the views of the U.S. DOE or the United States Government.

Notes and references

1 A. Muralidharan, M. I. Chaudhari, L. R. Pratt and S. B. Rempe, *Sci. Rep.*, 2018, **8**, 10736.

2 S. Varma, D. M. Rogers, L. R. Pratt and S. B. Rempe, *J. Gen. Phys.*, 2011, **137**, 479–488.

3 S. J. Percival, S. Russo, C. Priest, R. C. Hill, J. A. Ohlhausen, L. J. Small, S. B. Rempe and E. D. Spoerke, *Soft Matter*, 2021, **17**, 6315–6325.

4 D. S. Bolintineanu, M. Stevens and A. Frischknecht, *ACS Macro Letters*, 2013, **2**, 206–210.

5 D. S. Bolintineanu, M. Stevens and A. Frischknecht, *Macromolecules*, 2013, **46**, 5381.

6 M. P. Rosenwinkel, R. Andersson, J. Mindemark and M. Schönhoff, *J. Phys. Chem. C*, 2020, **124**, 23588–23596.

7 R. T. Cygan, C. J. Brinker, M. D. Nyman, K. Leung and S. B. Rempe, *MRS Bull.*, 2008, **33**, 42–47.

8 M. Elimelech and W. A. Phillip, *Science*, 2011, **333**, 712–717.

9 B. Hille, *Ionic Channels of Excitable Membranes*, Sinauer Associates: Sunderland, MA, 3rd edn, 2001.

10 E. Gouaux and R. MacKinnon, *Science*, 2005, **310**, 1461.

11 S. Varma and S. B. Rempe, *Biophys. J.*, 2007, **93**, 1093–1099.

12 B. Roux, *Essays Biochem.*, 2017, **61**, 201–209.

13 W. Chen, F.-Z. Liu, X.-Y. Feng, A. B. Djurišić, W. K. Chan and Z.-B. He, *Advanced Energy Materials*, 2017, **7**, 1700722.

14 B. J. Kim and G. Boschloo, *Nanoscale*, 2021, **13**, 11478–11487.

15 P. Hohenberg and W. Kohn, *Phys. Rev.*, 1964, **136**, B864–B871.

16 M. Stevens and S. Rempe, *J. Phys. Chem. B*, 2016, **120**, 12519–12530.

17 J. P. Glusker, *Adv. Prot. Chem.*, 1991, **42**, 1–76.

18 C. E. Valdez, Q. A. Smith, M. R. Nechay and A. N. Alexandrova, *Acc. Chem. Res.*, 2014, **47**, 3110–3117.

19 S. R. Sandler and W. Karo, *Polymer Synthesis*, Elsevier Inc, 2nd edn, 1996.

20 T. Baughman, C. Chan, K. Winey and K. Wagener, *Macromolecules*, 2007, **40**, 6564 – 6571.

21 L. Sauguet, F. Poitevin, S. Murail, C. Van Renterghem, G. Moraga-Cid, L. Malherbe, A. W. Thompson, P. Koehl, P. J. Corringer, M. Baaden and M. Delarue, *EMBO J.*, 2013, **32**, 728 – 741.

22 M. Seitz, C. Chan, K. Opper, T. Baughman, K. Wagener and K. Winey, *J. Am. Chem. Soc.*, 2010, **132**, 8165–8174.

23 D. L. Bostick and C. L. Brooks, *Proc. Natl. Acad. Sci.*, 2007, **104**, 9260–9265.

24 M. Thomas, D. Jayatilaka and B. Corry, *Biophys. J.*, 2007, **93**, 2635–2643.

25 S. Varma, D. Sabo and S. B. Rempe, *J. Molec. Biol.*, 2008, **376**, 13–22.

26 P. Jungwirth and P. S. Cremer, *Nature Chem.*, 2014, **6**, 261–263.

27 T. P. Pollard and T. L. Beck, *Curr. Opin. Coll. & Interf. Sci.*, 2016, **23**, 110–118.

28 H. I. Okur, J. Hladílková, K. B. Rembert, Y. Cho, J. Heyda, J. Dzubiella, P. S. Cremer and P. Jungwirth, *J. Phys. Chem. B*, 2017, **121**, 1997–2014.

29 G. Eisenman and R. Horn, *J. Membrane Biol.*, 1983, **76**, 197–225.

30 K. Collins, *Biophys. J.*, 1997, **72**, 65–76.

31 L. R. Pratt and S. B. Rempe, Simulation and Theory of Electro-

static Interactions in Solution, AIP Press, Vol. 492, New York, 1999, pp. 172–201.

32 D. M. Rogers, D. Jiao, L. Pratt and S. Rempe, *Ann. Rep. Comp. Chem.*, 2012, **8**, 71.

33 M. J. Frisch, G. W. Trucks, H. B. Schlegel, G. E. Scuseria, M. A. Robb, J. R. Cheeseman, G. Scalmani, V. Barone, G. A. Petersson, H. Nakatsuji, X. Li, M. Caricato, A. V. Marenich, J. Bloino, B. G. Janesko, R. Gomperts, B. Mennucci, H. P. Hratchian, J. V. Ortiz, A. F. Izmaylov, J. L. Sonnenberg, D. Williams-Young, F. Ding, F. Lipparini, F. Egidi, J. Goings, B. Peng, A. Petrone, T. Henderson, D. Ranasinghe, V. G. Zakrzewski, J. Gao, N. Rega, G. Zheng, W. Liang, M. Hada, M. Ehara, K. Toyota, R. Fukuda, J. Hasegawa, M. Ishida, T. Nakajima, Y. Honda, O. Kitao, H. Nakai, T. Vreven, K. Throssell, J. A. Montgomery, Jr., J. E. Peralta, F. Ogliaro, M. J. Bearpark, J. J. Heyd, E. N. Brothers, K. N. Kudin, V. N. Staroverov, T. A. Keith, R. Kobayashi, J. Normand, K. Raghavachari, A. P. Rendell, J. C. Burant, S. S. Iyengar, J. Tomasi, M. Cossi, J. M. Millam, M. Klene, C. Adamo, R. Cammi, J. W. Ochterski, R. L. Martin, K. Morokuma, O. Farkas, J. B. Foresman and D. J. Fox, *Gaussian 16 Revision C.01*, 2016, Gaussian Inc. Wallingford CT.

34 A. Becke, *J. Chem. Phys.*, 1998, **98**, 1372.

35 K. A. Peterson and T. H. Dunning, *J. Chem. Phys.*, 2002, **117**, 10548.

36 J. G. Hill and K. A. Peterson, *The Journal of Chemical Physics*, 2017, **147**, 244106.

37 M. Tafipolsky and R. Schmid, *J. Chem. Theo. Comp.*, 2009, **5**, 2822–2834.

38 J. Oomens and J. D. Steill, *J. Phys. Chem. A*, 2008, **112**, 3281–3283.

39 K. Burke, *J. Chem. Phys.*, 2012, **136**, 150901.

40 J.-D. Chai and M. Head-Gordon, *Phys. Chem. Chem. Phys.*, 2008, **10**, 6615–6620.

41 M. Soniat, D. M. Rogers and S. B. Rempe, *J. Chem. Theory Comput.*, 2015, 2958–2967.

42 P. Hay and W. Wadt, *J. Chem. Phys.*, 1985, **82**, 270.

43 S. B. Rempe and H. Jónsson, *Chem. Educ.*, 1998, **3**, 1–17.

44 W. Humphrey, A. Dalke and K. Schulten, *Journal of Molecular Graphics*, 1996, **14**, 33–38.

45 L.-Y. Hsu and C. E. Nordman, *Acta Crystallographica Section C*, 1983, **39**, 690–694.

46 A. Lossin and G. Meyer, *Zeitschrift für anorganische und allgemeine Chemie*, 1993, **619**, 1462–1464.

47 F. J. Martínez Casado, M. Ramos Riesco, M. I. Redondo, D. Choquesillo-Lazarte, S. López-Andrés and J. A. R. Cheda, *Crystal Growth & Design*, 2011, **11**, 1021–1032.

48 K. Shigenobu, M. Shibata, K. Dokko, M. Watanabe, K. Fujii and K. Ueno, *Phys. Chem. Chem. Phys.*, 2021, **23**, 2622–2629.

49 G. G. Eshetu, D. Mecerreyes, M. Forsyth, H. Zhang and M. Armand, *Mol. Syst. Des. Eng.*, 2019, **4**, 294–309.

50 R. Hilf and R. Dutzler, *Nature*, 2009, **457**, 115–118.

51 H. Kato, F. Zhang, O. Yizhar, C. Ramakrishnan, T. Nishizawa, K. Hirata, J. Ito, Y. Aita, T. Tsukazaki, S. Hayashi, P. Hegemann, A. Maturana, R. Ishitani, K. Deisseroth and O. Nureki, *Nature*, 2012, **482**, 369.

52 R. Salari, S. Murlidaran and G. Brannigan, *Mol. Simul.*, 2014, **40**, 821–829.

53 C. Öster, K. Hendricks, W. Kopec, V. Chevelkov, C. Shi, D. Michl, S. Lange, H. Sun, B. L. deGroot and A. Lange, *Sci. Adv.*, 2019, **5**, 1–8.

54 S. E. Strong, N. J. Hestand, A. A. Kananenka, M. T. Zanni and J. Skinner, *Biophys. J.*, 2020, **118**, 254–261.

55 M. R. VanGordon, L. A. Prignano, R. E. Dempski, S. W. Rick and S. B. Rempe, *Biophys. J.*, 2021, **120**, 1835–1845.

56 T. Negoro, K. Hirata, J. M. Lisy, S.-i. Ishiuchi and M. Fujii, *Phys. Chem. Chem. Phys.*, 2021, **23**, 12045–12050.

57 Z. Jing, J. A. Rackers, L. Pratt, C. Liu, S. B. Rempe and P. Ren, *Chem. Sci.*, 2021, **12**, 8920.

58 D. Mendes de Oliveira, S. R. Zukowski, V. Palivec, J. Hénin, H. Martinez-Seara, D. Ben-Amotz, P. Jungwirth and E. Duboué-Dijon, *Phys. Chem. Chem. Phys.*, 2020, **22**, 24014–24027.